

# On the use of the KMR unintegrated parton distribution functions

---

Krzysztof Golec-Biernat<sup>a,b</sup> Anna M. Staśto<sup>c</sup>

<sup>a</sup>*Institute of Nuclear Physics, Polish Academy of Sciences, 31-342 Cracow, Poland*

<sup>b</sup>*Faculty of Mathematics and Natural Sciences, University of Rzeszów, 35-959 Rzeszów, Poland*

<sup>c</sup>*Department of Physics, The Pennsylvania State University, University Park, PA 16802, U.S.A.*

*E-mail:* [golec@ifj.edu.pl](mailto:golec@ifj.edu.pl), [astasto@phys.psu.edu](mailto:astasto@phys.psu.edu)

**ABSTRACT:** We discuss the unintegrated parton distribution functions (UPDFs) introduced by Kimber, Martin and Ryskin (KMR), which are frequently used in phenomenological analyses of hard processes with transverse momenta of partons taken into account. We demonstrate numerically that the commonly used differential definition of the UPDFs leads to erroneous results for large transverse momenta. We identify the reason for that, being the use of the ordinary PDFs instead of the cutoff dependent distribution functions. We show that in phenomenological applications, the integral definition of the UPDFs with the ordinary PDFs can be used.

**KEYWORDS:** Quantum Chromodynamics, parton distributions, transverse momentum dependence, evolution equations

---

## Contents

|          |  |          |
|----------|--|----------|
| <b>1</b> | <b>Introduction</b>                      | <b>1</b> |
| <b>2</b> | <b>Unintegrated parton distributions</b> | <b>2</b> |
| <b>3</b> | <b>Discussion of the cutoff</b>          | <b>4</b> |
| <b>4</b> | <b>Numerical analysis</b>                | <b>5</b> |
| <b>5</b> | <b>Cutoff dependent PDFs</b>             | <b>6</b> |
| <b>6</b> | <b>Conclusions</b>                       | <b>8</b> |

---

## 1 Introduction

The standard description of hard processes in Quantum Chromodynamics relies on the collinear factorization theorems [1, 2]. In this approach, the short distance physics is incorporated in the perturbatively calculable partonic matrix elements and the information about hadron structure, including the long-distance physics, is encoded in the integrated parton distribution functions (PDFs). These distributions depend on the fraction  $x$  of the hadron longitudinal momentum carried by a parton and on a scale  $Q$  of the hard process. The PDFs satisfy the perturbative DGLAP evolution equations [3–5], which allow to evaluate them at the scale  $Q$  once the initial conditions, parametrizing non-perturbative physics at some lower scale,  $Q_0 < Q$ , are given.

However, such a description may not be satisfactory for some exclusive processes. They may require more precise information about parton kinematics, in particular, about the transverse momenta of incoming partons participating in the collision, see for example [6, 7]. Such corrections are in principle encoded in the higher order perturbative terms to the partonic matrix elements, but the alternative approach is to use the formalism where the parton distributions include the dependence on the transverse momentum in addition to the longitudinal momentum fraction. This can be done by using the so-called unintegrated parton distribution functions (UPDFs). There are number of approaches which incorporate the transverse momentum dependence in the parton distributions: high energy or small  $x$  formalism, for example the BFKL [8–10] or CCFM [11–14] equations used in the  $k_T$  factorization [15] or the CSS evolution [16] and the related TMD factorization [2].

A popular way to obtain the UPDFs is to use the formalism proposed by Martin, Kimber and Ryskin (KMR) [17, 18]. In this approach, one can obtain the UPDFs from the integrated PDFs and the Sudakov form factors (see [19, 20] for the Monte Carlo implementation of parton branching from DGLAP evolution). Usually, the differential formula

is used where the UPDFs are obtained by taking the derivative of the integrated PDFs

$$f_a(x, k_\perp, Q) = \frac{\partial}{\partial \ln k_\perp^2} [T_a(Q, k_\perp) D_a(x, k_\perp)], \quad (1.1)$$

where  $T_a$  is the Sudakov form factor and  $D_a(x, k_\perp)$  is the integrated parton distribution. This prescription is widely used in phenomenological analyses presented in the literature. It turns out however, that such a prescription leads to some unphysical results for large values of transverse momenta,  $k_\perp \geq Q$ . For example, we find negative or discontinuous UPDFs in one of the two discussed approximations, when the differential formula (1.1) is used. We identified the reason for such a behaviour and show how to compute the UPDFs which are free of such problems.

This paper is organized as follows. In Sec. 2 we recall the KMR construction leading to the differential and integral forms of the UPDFs. In Sec. 3 we discuss two choices of the cutoff, used in the literature. In Sec. 4 we perform the numerical analysis, and illustrate the specific problems with the differential formula for the UPDFs. In Sec. 5 we show the equivalence between the differential and integral forms of the UPDFs using cutoff dependent integrated PDFs. Finally, in Sec. 6 we state our conclusions.

## 2 Unintegrated parton distributions

The starting point for the derivation of the KMR UPDFs in [17, 18] are the DGLAP evolution equations for the integrated parton distributions  $D_a(x, \mu)$

$$\frac{\partial D_a(x, \mu)}{\partial \ln \mu^2} = \sum_{a'} \int_x^{1-\Delta} \frac{dz}{z} P_{aa'}(z, \mu) D_{a'}\left(\frac{x}{z}, \mu\right) - D_a(x, \mu) \sum_{a'} \int_0^{1-\Delta} dz z P_{a'a}(z, \mu) \quad (2.1)$$

where  $a$  denotes quark flavour/antiflavour or gluon and  $P_{aa'}$  are the Altarelli-Parisi splitting functions

$$P_{aa'}(z, \mu) = \frac{\alpha_s(\mu)}{2\pi} P_{aa'}^{(LO)}(z). \quad (2.2)$$

We will consider here LO approximation, but the analysis can be extended to higher orders. The two integrals in Eq. (2.1) are separately divergent for  $\Delta = 0$  due to the singular splitting functions  $P_{qq}$  and  $P_{gg}$  at  $z = 1$ . The first term describes the real emissions in the region  $\mu^2 < k_\perp^2 < \mu^2 + \delta\mu^2$ , where  $k_\perp$  is the transverse momentum of the exchanged parton, whereas the second term is responsible for the virtual emissions. In the DGLAP equations these singularities, which are due to soft emissions, cancel when the two terms are combined, through the plus prescription. However, by introducing a parameter  $\Delta$ , one is able to separate the positive real emission term from the negative virtual emission one, which allows further manipulations leading to the definition of the UPDFs. In particular the choice of the cutoff will be physically motivated, and it will reflect the ordering of the parton emissions.

Let us take for the factorization scale the exchanged parton transverse momentum,  $\mu = |\mathbf{k}_\perp| \equiv k_\perp$ , and rewrite Eq. (2.1) in the form

$$\frac{\partial D_a(x, k_\perp)}{\partial \ln k_\perp^2} + D_a(x, k_\perp) \sum_{a'} \int_0^{1-\Delta} dz z P_{a'a}(z, k_\perp) = \sum_{a'} \int_x^{1-\Delta} \frac{dz}{z} P_{aa'}(z, k_\perp) D_{a'}\left(\frac{x}{z}, k_\perp\right). \quad (2.3)$$

Let us also introduce the Sudakov formfactor

$$T_a(Q, k_\perp) = \exp \left\{ - \int_{k_\perp^2}^{Q^2} \frac{dp_\perp^2}{p_\perp^2} \sum_{a'} \int_0^{1-\Delta} dz z P_{a'a}(z, p_\perp) \right\}, \quad (2.4)$$

which has the interpretation of the probability that the parton with transverse momentum  $k_\perp$  will survive (without splitting) up to the factorization scale  $Q$ . After multiplying both sides of Eq. (2.3) by the Sudakov form factor, the l.h.s. can be written as a full derivative,

$$\frac{\partial}{\partial \ln k_\perp^2} [T_a(Q, k_\perp) D_a(x, k_\perp)] = T_a(Q, k_\perp) \sum_{a'} \int_x^{1-\Delta} \frac{dz}{z} P_{aa'}(z, k_\perp) D_{a'}\left(\frac{x}{z}, k_\perp\right). \quad (2.5)$$

Integrating both sides of the above equation over  $k_\perp$  in the interval  $[Q_0, Q]$ , where  $Q_0$  is an initial scale for the DGLAP evolution, we find on the l.h.s.

$$\int_{Q_0^2}^{Q^2} \frac{dk_\perp^2}{k_\perp^2} \frac{\partial}{\partial \ln k_\perp^2} [T_a(Q, k_\perp) D_a(x, k_\perp)] = D_a(x, Q) - T_a(Q, Q_0) D_a(x, Q_0), \quad (2.6)$$

since  $T_a(Q, Q) = 1$ . Thus, Eq. (2.5) takes the following form

$$D_a(x, Q) = T_a(Q, Q_0) D_a(x, Q_0) + \int_{Q_0^2}^{Q^2} \frac{dk_\perp^2}{k_\perp^2} \left\{ T_a(Q, k_\perp) \sum_{a'} \int_x^{1-\Delta} \frac{dz}{z} P_{aa'}(z, k_\perp) D_{a'}\left(\frac{x}{z}, k_\perp\right) \right\}. \quad (2.7)$$

This form of Eq. (2.1) may serve as a basis for Monte Carlo simulations of parton branching processes, see for example [21].

The expression in the curly brackets in Eq. (2.7) defines the unintegrated parton distribution functions,

$$f_a(x, k_\perp, Q) \equiv T_a(Q, k_\perp) \sum_{a'} \int_x^{1-\Delta} \frac{dz}{z} P_{aa'}(z, k_\perp) D_{a'}\left(\frac{x}{z}, k_\perp\right), \quad (2.8)$$

which are given in the range  $k_\perp \geq Q_0$ . Notice that with this definition, the UPDFs are dimensionless quantities as there are the PDFs. By the comparison of Eqs. (2.5) and (2.8) we can also write

$$f_a(x, k_\perp, Q) = \frac{\partial}{\partial \ln k_\perp^2} [T_a(Q, k_\perp) D_a(x, k_\perp)]. \quad (2.9)$$

Formula (2.9) is commonly used to construct the UPDFs from the integrated PDFs, and is referred to as the KMR prescription [17, 18]. The discussion of its applicability is the main subject of this paper.

For  $k_\perp < Q_0$  we need modeling, for example the UPDFs can be defined as below

$$f_a(x, k_\perp, Q) = f_a(x, Q_0, Q) \frac{k_\perp^2}{Q_0^2}. \quad (2.10)$$

Thus, we assume a constant behaviour of the distribution  $f_a(x, k_\perp, Q)/k_\perp^2$  as a function of the transverse momentum.

### 3 Discussion of the cutoff

In Ref. [17] the cutoff  $\Delta$  was set in accordance with the strong ordering (SO) in transverse momenta of the real parton emission in the DGLAP evolution,

$$\Delta = \frac{k_\perp}{Q}. \quad (3.1)$$

In the Sudakov form factor (2.4),  $k_\perp$  is replaced by the loop momentum  $p_\perp$ , and

$$T_a(Q, k_\perp) = \exp \left\{ - \int_{k_\perp^2}^{Q^2} \frac{dp_\perp^2}{p_\perp^2} \sum_{a'} \int_0^{1-\Delta(p_\perp)} dz z P_{a'a}(z, p_\perp) \right\}, \quad (3.2)$$

where  $\Delta(p_\perp) = p_\perp/Q$ . Since the integration limits in the real emission term in Eq. (2.8) should obey the condition  $x < (1 - \Delta)$ , the UPDFs are nonzero only for the transverse momenta

$$k_\perp \leq Q(1 - x). \quad (3.3)$$

With such a prescription, we always have  $k_\perp < Q$  and  $T_a(Q, k_\perp) < 1$ .

The prescription for the cutoff  $\Delta$  was further modified in Ref. [18, 22] to account for the angular ordering (AO) in parton emissions in the sprint of the CCFM evolution [11–14],

$$\Delta = \frac{k_\perp}{k_\perp + Q}. \quad (3.4)$$

In such a case, the nonzero values of the UDPFs are given for

$$k_\perp \leq Q \left( \frac{1}{x} - 1 \right). \quad (3.5)$$

The upper limit for  $k_\perp$  is now bigger than in the DGLAP scheme. This is particularly important for small values of  $x$ , when  $k_\perp < Q/x$ , which allows for a smooth transition of transverse momenta into the region  $k_\perp \gg Q$ , see Ref. [18, 22] for more details. In this region, we have to decide on the form of the Sudakov form factor (3.2) in which  $\Delta(p_\perp) = p_\perp/(p_\perp + Q)$ . For  $k_\perp > Q$ , the integration gives a negative value and  $T_a(Q, k_\perp) > 1$ , which contradicts the interpretation of the Sudakov form factor as a probability of no real emission. In the usual approach, the Sudakov form factor is frozen to one

$$T_a(Q, k_\perp) = 1, \quad k_\perp > Q. \quad (3.6)$$

Notice that with such a prescription,  $T_a$  has the first derivative discontinuous at  $k_\perp = Q$ . This effect will be seen in our numerical analysis.

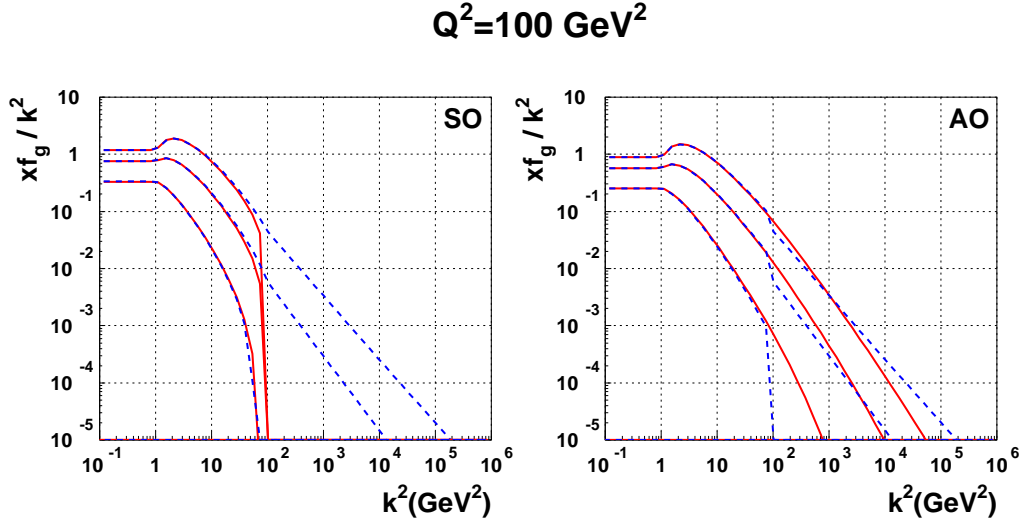


**Figure 1.** The unintegrated gluon distribution  $x f_g(x, k_\perp, Q)/k_\perp^2$  as a function of  $k^2 \equiv k_\perp^2$  for  $x = 10^{-3}, 10^{-2}, 10^{-1}$  (from top to bottom). The solid curves are obtained from Eq. (2.8) while the dashed ones from Eq. (2.9). The plot on the left shows the unintegrated gluon distribution with the SO cutoff (3.1) while the plot on the right the gluon distribution with the AO cutoff (3.4).

#### 4 Numerical analysis

Let us discuss the problem of the equivalence of the definitions (2.8) and (2.9) of the UPDFs. For the illustration, we use the unintegrated gluon distribution which is computed in the complete approach with quarks. The integrated PDFs in our numerical analysis are computed using the MSTW08 parametrization [23] of the initial conditions for the DGLAP evolution equations.

In Fig. 1 we show the unintegrated gluon distribution  $x f_g(x, k_\perp, Q)/k_\perp^2$  as a function of  $k_\perp^2$  for  $Q^2 = 100 \text{ GeV}^2$  and  $x = 10^{-3}, 10^{-2}, 10^{-1}$  (from the top to the bottom) in the strong ordering (SO) (left plot) and angular ordering (AO) (right plot) approximations for the cutoff  $\Delta$ . The solid lines are obtained from the integral form (2.8) while the dashed ones are from the differential formula (2.9).

In the SO case, shown on the left, we see a sharp cutoff for the solid curves resulting from condition (3.3). Such a cutoff is not present for the dashed curves computed from Eq. (2.9), which go into the forbidden region,  $k_\perp > Q$ . In this region

$$f_g(x, k_\perp, Q) = \frac{\partial}{\partial \ln k_\perp^2} [D_g(x, k_\perp)] \quad (4.1)$$

due to condition (3.6), and the integrated gluon distribution on the r.h.s. has no limitations on the maximal value of the hard scale  $k_\perp$ . Clearly, such a behaviour contradicts the assumption on the SO approximation.

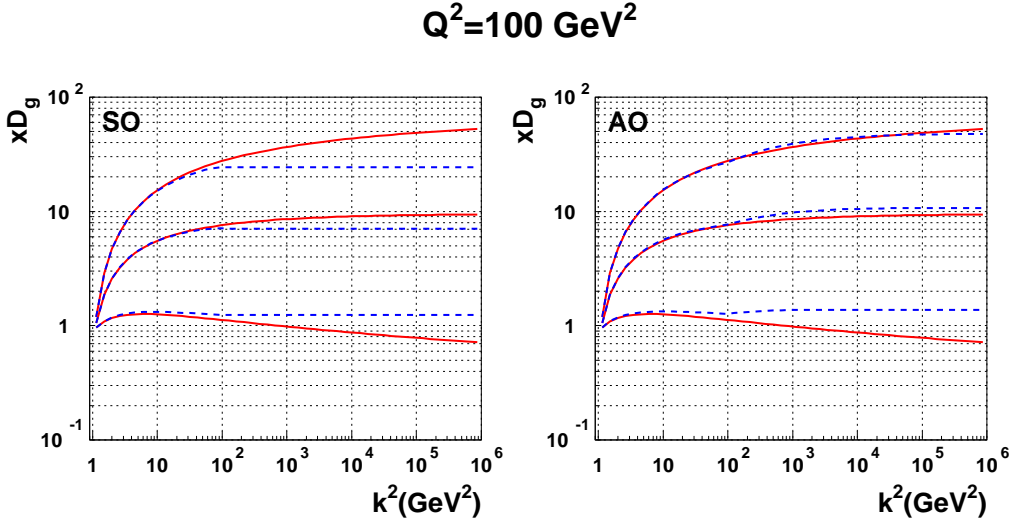


**Figure 2.** The cutoff dependent integrated gluon distribution,  $xD_g(x, k_\perp, \Delta)$ , as a function of  $k^2 \equiv k_\perp^2$  for  $x = 10^{-3}, 10^{-2}, 10^{-1}$  (from top to bottom), found from Eq. (2.5) (dashed lines), versus the gluon distribution from the ordinary DGLAP equations (solid lines). The results in the SO and AO approximations are shown.

In the AO case, shown on the right plot in Fig. 1, the distributions from the integral formula (2.8) (solid lines) extend far beyond the point  $k_\perp = Q$ , due to relation (3.5). The unphysical discontinuity at  $k_\perp = Q$  of the distributions from the differential formula (2.9) (dashed lines) is a result of the discontinuity of the first derivative of the Sudakov form factor at this point. Notice also that the lowest lying dashed curve, which corresponds to  $x = 10^{-1}$ , drops abruptly at  $k_\perp = Q$ . For such a value of  $x$ , the integrated gluon distribution  $D_g(x, k_\perp)$  decreases with rising  $k_\perp$ , and its derivative (4.1) becomes negative ( $\sim -10^{-2}$ ) which leads to a sharp drop on the logarithmic plot. On the other hand, the curves obtained from the integral formula behave in a smooth way without any discontinuities.

## 5 Cutoff dependent PDFs

An important question arises here, why the formulae (2.8) and (2.9) for the UPDFs give different results despite their seemingly mathematical equivalence. To answer this question, we have to realize that the equivalence crucially depends on the existence of the cutoff  $\Delta$ . To compute the UPDFs, we have to solve first Eq. (2.1) (or its equivalent form (2.5)) which gives the cutoff dependent integrated PDFs,  $D_a(x, k_\perp, \Delta)$ . With such distributions, the UPDFs from Eqs. (2.8) and (2.9) will be the same. However, in the numerical analysis in the previous section, we follow the standard approach with the PDFs obtained from the DGLAP evolution equations with  $\Delta = 0$ , in which the singularity at  $z = 1$  is regularized

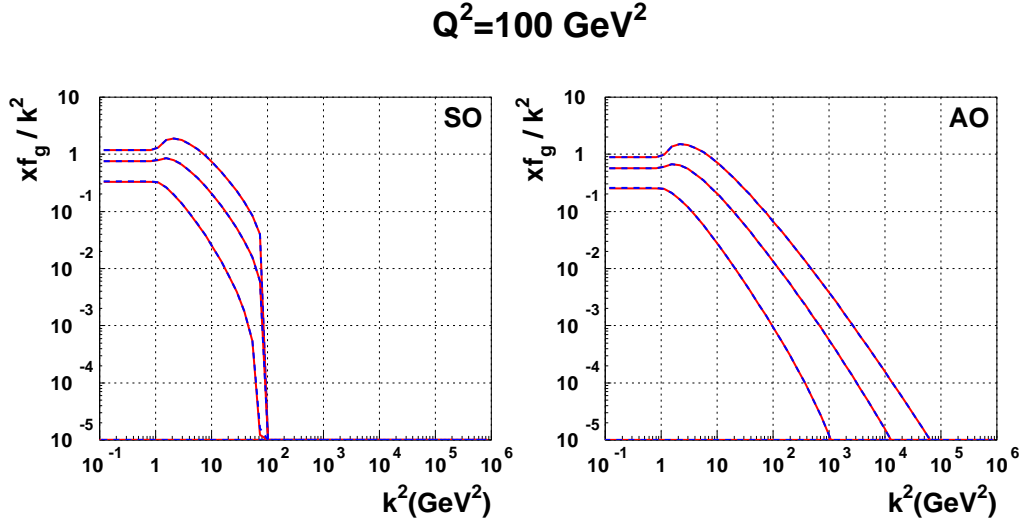


**Figure 3.** The unintegrated gluon distribution  $xf_g(x, k_\perp, Q)/k_\perp^2$  as a function of  $k^2 \equiv k_\perp^2$  for  $x = 10^{-3}, 10^{-2}, 10^{-1}$  (from top to bottom) in the SO and AO cases, found with the help of the cutoff dependent PDFs. The solid curves are from Eq. (2.8) while the dashed ones from Eq. (2.9).

by the plus prescription. This is why we find different results for the UPDFs from the two prescriptions.

In order to demonstrate this effect, we solve Eq. (2.5) with the cutoffs in the SO and AO cases. We also use prescription (3.6) for the values of the Sudakov form factor for  $k_\perp > Q$ . In Fig. 2 we show, as an example, the cutoff dependent integrated gluon distribution,  $x D_g(x, k_\perp, \Delta)$ , as a function of the factorization scale  $k_\perp^2$  for  $Q^2 = 100 \text{ GeV}^2$  (dashed lines). The ordinary gluon distribution obtained from the DGLAP equations with  $\Delta = 0$  is shown as the solid lines. In the SO case (left plot), we plot the cutoff dependent distribution in the forbidden region,  $k_\perp > Q$ , which is equal to a constant since the r.h.s of Eq. (2.5) vanishes there. Thus, the unintegrated gluon distribution equals zero in this region, which is clearly seen on the left plot in Fig. 3 where we plot the UPDFs obtained from the cutoff dependent PDFs in the SO approximation.

Now, we can check that the integral and differential prescriptions for the unintegrated gluon distributions are exactly equivalent, provided the cutoff dependent integrated parton densities are used. This is seen in Fig. 3, where we demonstrate the equality of the results on the unintegrated gluon distribution,  $xf_g(x, k_\perp, Q)/k_\perp^2$ , obtained from the integral and differential prescriptions of the UPDFs.

Since the parametrizations of the integrated PDFs are only available for the cutoff independent case, it is important to check how numerically big is the effect of the cutoff on the unintegrated distributions. In Fig. 4, we show the comparison of the unintegrated gluon distributions computed from the integral formula (2.8) in the SO and AO cases. The



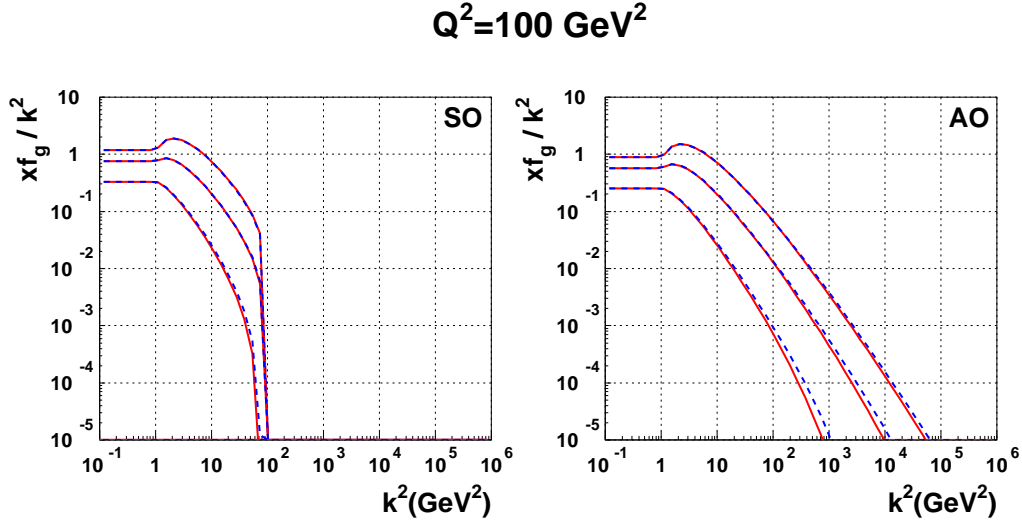


**Figure 4.** The comparison of the unintegrated gluon distributions,  $xf_g(x, k_\perp, Q)/k_\perp^2$ , computed from the integral formula (2.8) for  $x = 10^{-3}, 10^{-2}, 10^{-1}$  (from top to bottom) in the SO and AO cases. The solid curves show the results obtained with the ordinary PDFs while the dashed curves are found with the cutoff dependent PDFs.

solid curves show the results obtained with the ordinary integrated PDFs while the dashed curves are found with the cutoff dependent parton distributions. As we see, the difference is marginal. Therefore, the standard procedure to compute the UPDFs from the ordinary PDFs is acceptable as long as the integral definition (2.8) is used. The differential form (2.9), however, causes problems for large values of transverse momenta,  $k_\perp \sim Q$  and should be avoided.

## 6 Conclusions

We critically re-examined the derivation and hidden assumptions leading to the UPDFs proposed by Kimber, Martin and Ryskin [17, 18], which are commonly used in the phenomenological analyses with parton distributions which additionally depend on parton transverse momentum,  $k_\perp$ . We found that in the standard approach, when the ordinary PDFs found from the global fits to data are used, the definitions (2.8) and (2.9) of the UPDFs give different results in the large transverse momentum region,  $k_\perp \sim Q$ . In particular, the UPDFs from the differential formula (2.9) extends in the SO approximation into the forbidden region,  $k_\perp \geq Q$ , and are discontinuous or negative in this region in the AO approximation.

We identified the reason for such a pathological behaviour, being the use of the ordinary PDFs instead of the the cutoff dependent PDFs which guarantee the mathematical equivalence of the two definitions of UPDFs. We demonstrated such an equivalence nu-

merically, using the equation (2.1) with the cutoff  $\Delta$  in the SO and AO approximations. With the cutoff dependent PDFs, the UPDFs no longer suffer from the described above pathological behaviour.

However, the use of the cutoff dependent PDFs is cumbersome and might spoil the effectiveness of the phenomenological analyses with the KMR UPDFs. The good news is that the UPDFs computed from the formula (2.8) are practically the same, regardless of the choice of the ordinary or cutoff dependent PDFs in the calculations. Thus, as a final conclusion, the KMR UPDFs should only be computed from the integral formula (2.8) in which the PDFs from the global fits can be used.

## Acknowledgments

This work was supported by the Department of Energy Grant No. DE-SC-0002145 and by the National Science Center, Poland, Grant No. 2015/17/B/ST2/01838. We thank Krzysztof Kutak for discussions.

## References

- [1] J. C. Collins, D. E. Soper and G. F. Sterman, *Factorization of Hard Processes in QCD*, *Adv. Ser. Direct. High Energy Phys.* **5** (1989) 1–91, [[hep-ph/0409313](#)].
- [2] John Collins, *Foundations of perturbative QCD*, vol. 32. Cambridge Univ. Press, 2011.
- [3] V. N. Gribov and L. N. Lipatov, *Deep inelastic  $e p$  scattering in perturbation theory*, *Sov. J. Nucl. Phys.* **15** (1972) 438–450.
- [4] G. Altarelli and G. Parisi, *Asymptotic Freedom in Parton Language*, *Nucl. Phys.* **B126** (1977) 298–318.
- [5] Y. L. Dokshitzer, *Calculation of the Structure Functions for Deep Inelastic Scattering and  $e+ e-$  Annihilation by Perturbation Theory in Quantum Chromodynamics.*, *Sov. Phys. JETP* **46** (1977) 641–653.
- [6] J. Collins and H. Jung, *Need for fully unintegrated parton densities*, in *HERA and the LHC: A Workshop on the implications of HERA for LHC physics. Proceedings, Part B*, 2005. [[hep-ph/0508280](#)].
- [7] J. C. Collins, T. C. Rogers and A. M. Stasto, *Fully unintegrated parton correlation functions and factorization in lowest-order hard scattering*, *Phys. Rev.* **D77** (2008) 085009, [[0708.2833](#)].
- [8] E. A. Kuraev, L. N. Lipatov and V. S. Fadin, *Multi - Reggeon Processes in the Yang-Mills Theory*, *Sov. Phys. JETP* **44** (1976) 443–450.
- [9] E. A. Kuraev, L. N. Lipatov and V. S. Fadin, *The Pomeron Singularity in Nonabelian Gauge Theories*, *Sov. Phys. JETP* **45** (1977) 199–204.
- [10] I. I. Balitsky and L. N. Lipatov, *The Pomeron Singularity in Quantum Chromodynamics*, *Sov. J. Nucl. Phys.* **28** (1978) 822–829.
- [11] M. Ciafaloni, *Coherence Effects in Initial Jets at Small  $q^2/s$* , *Nucl. Phys.* **B296** (1988) 49–74.
- [12] S. Catani, F. Fiorani and G. Marchesini, *Small  $x$  Behavior of Initial State Radiation in Perturbative QCD*, *Nucl. Phys.* **B336** (1990) 18–85.
- [13] S. Catani, F. Fiorani and G. Marchesini, *QCD Coherence in Initial State Radiation*, *Phys. Lett.* **B234** (1990) 339–345.
- [14] G. Marchesini, *QCD coherence in the structure function and associated distributions at small  $x$* , *Nucl. Phys.* **B445** (1995) 49–80, [[hep-ph/9412327](#)].
- [15] S. Catani, M. Ciafaloni and F. Hautmann, *High-energy factorization and small  $x$  heavy flavor production*, *Nucl. Phys.* **B366** (1991) 135–188.
- [16] J. C. Collins, D. E. Soper and G. F. Sterman, *Transverse Momentum Distribution in Drell-Yan Pair and  $W$  and  $Z$  Boson Production*, *Nucl. Phys.* **B250** (1985) 199–224.
- [17] M. A. Kimber, A. D. Martin and M. G. Ryskin, *Unintegrated parton distributions and prompt photon hadroproduction*, *Eur. Phys. J.* **C12** (2000) 655–661, [[hep-ph/9911379](#)].
- [18] M. A. Kimber, A. D. Martin and M. G. Ryskin, *Unintegrated parton distributions*, *Phys. Rev.* **D63** (2001) 114027, [[hep-ph/0101348](#)].
- [19] F. Hautmann, H. Jung, A. Lelek, V. Radescu and R. Zlebcik, *Soft-gluon resolution scale in QCD evolution equations*, *Phys. Lett.* **B772** (2017) 446–451, [[1704.01757](#)].

- [20] F. Hautmann, H. Jung, A. Lelek, V. Radescu and R. Zlebcik, *Collinear and TMD Quark and Gluon Densities from Parton Branching Solution of QCD Evolution Equations*, *JHEP* **01** (2018) 070, [[1708.03279](#)].
- [21] K. J. Golec-Biernat, S. Jadach, W. Placzek and M. Skrzypek, *Markovian Monte Carlo solutions of the NLO QCD evolution equations*, *Acta Phys. Polon.* **B37** (2006) 1785–1832, [[hep-ph/0603031](#)].
- [22] M. A. Kimber, J. Kwiecinski, A. D. Martin and A. M. Stasto, *The Unintegrated gluon distribution from the CCFM equation*, *Phys. Rev.* **D62** (2000) 094006, [[hep-ph/0006184](#)].
- [23] A. Martin, W. Stirling, R. Thorne and G. Watt, *Parton distributions for the LHC*, *Eur.Phys.J.* **C63** (2009) 189–285, [[0901.0002](#)].